

# DSC and spectroscopic studies of the structure of $V_2O_5$ – $CdO$ – $P_2O_5$ glasses

N. KERKOURI\*, M. ET-TABIROU, A. CHAHINE, A. MAZZAH<sup>a</sup>, M. C. DHAMELINCOURT<sup>a</sup>, M. TAIBI<sup>b</sup>

*Laboratoire de Physico-Chimie des Matériaux Vitreux et Cristallisés (LPCMVC), Faculté des Sciences, Université Ibn Tofail, BP 133, Kenitra 14000, Morocco*

*<sup>a</sup>Laboratoire de Spectrochimie Infrarouge et Raman, CNRS UMR 8516, Bât C5, Université des Sciences et Technologies de Lille, 59655 Villeneuve d'asq Cedex, France*

*<sup>b</sup>Laboratoire de Physico-Chimie des Matériaux, Associé à l'AUF (LAF 502), ENS Takaddoum, BP 5118, Rabat 10000, Morocco*

$xV_2O_5$ – $(50-x)CdO$ – $50P_2O_5$  ( $0 \leq x \leq 50$  mol%) glasses were prepared and investigated using DSC, IR spectroscopy and Raman spectroscopy. For low concentrations of  $V_2O_5$  ( $x \leq 20$  mol %), the formation of P–O–V bonds increases the cross-link strength of the glass network and leads to increased  $T_g$ . For  $x > 20$  mol%, the infrared and Raman spectra show that the vanadium–oxygen structural units formed in the glasses are  $VO_5$  and  $VO_4$  groups forming chains with V–O–V bridges. The formation of the weaker V–O–V bonds compared with the stronger P–O–P bonds leads to decreased  $T_g$ .

(Received March 2, 2010; accepted May 26, 2010)

*Keywords:* Glasses,  $V_2O_5$ – $CdO$ – $P_2O_5$ , DSC, Infrared spectroscopy, Raman spectroscopy

## 1. Introduction

$P_2O_5$  is considered as one of the glass forming oxides whereas  $V_2O_5$  is a conditional glass former [1]. Growing attention has been given in the last decade to phosphate glasses containing  $V_2O_5$  [2-6]. There is a considerable practical interest in these glasses due to their optical properties [7] and their electrical properties [8-10]. The structure of these glasses has been the object of different studies. The determination of structure of amorphous solids is a difficult task and usually requires a combination of experimental techniques. Thus, for vanadophosphate glasses, EXAFS [11], XANES [12] and Raman spectroscopy [2, 4] have shown the presence of  $VO_4$  and/or  $VO_5$  and  $PO_4$  units which are connected to each other via oxygen bridges to form a three dimensional network. The structural role of  $V_2O_5$  in many oxide glasses is known to play a dual structural role both as a network modifier and as a network former [13].  $V_2O_5$  when mixed with glass former like  $B_2O_3$ ,  $P_2O_5$ ,  $TeO_2$  form stable glasses in comparatively wide range of compositions [14]. The studies on glasses containing  $CdO$  and  $V_2O_5$  together are few [15-17]. These types of glasses have gained special interest because of their mixed electronic (via electron hopping between  $V^{4+}$  and  $V^{5+}$  ions) and ionic (via  $Cd^{2+}$  ions) conductivity [15]. In the present paper we report the results of a study of the relationship between the structure and glass transition temperature of  $V_2O_5$ – $CdO$ – $P_2O_5$  glass system with the aid of infrared spectroscopy and Raman spectroscopy.

## 2. Experimental procedure

The  $xV_2O_5$ – $(50-x)CdO$ – $50P_2O_5$  samples were prepared from stoichiometric powders resulting from the mixing of  $CdCO_3$ ,  $V_2O_5$  and  $(NH_4)_2HPO_4$  ( $0 \leq x \leq 50$  mol%  $V_2O_5$ ). The oxidation and reduction reactions in a glass melt are known to depend on the size of the melt, the sample geometry, the concentration of total redox ions, thermal history and quenching rate [18, 19]. To keep these parameters constant, all glass samples were prepared under the same conditions as follow.

After mixing a batch of about 12 g with prescribed compositions, the mixed mass of each glass composition was melted in an alumina crucible for 2 h at 500 °C in an electric furnace in order to evaporate ammonia, carbonate and water in the batch, and minimize the tendency of subsequent phosphate loss. Next, the temperature was raised gradually to 1000 °C and held constant at this value for 30 min to homogenize the melt. The molten glasses were then quenched to room temperature under air atmosphere. The glasses were then stored under vacuum in a desiccator over silica gel until use.

## 3. Characterization procedure

The X-ray diffraction (XRD) patterns of the samples were recorded using a Philips (X'PERT- PRO) diffractometer. The glass transition temperatures ( $T_g$ ) were determined using differential scanning calorimeter (DSC SETARAM 121) at heating rate of (10 °C.min<sup>-1</sup>) under argon atmosphere, these temperatures are reproducible to  $\pm 5$  °C.

The IR spectra of the samples were recorded at room temperature in the range  $400$ – $1400\text{ cm}^{-1}$  by the standard KBr pellet disc method using a Fourier transform infrared (FT-IR) spectrometer (BRUCKER Tensor 27). The glass samples were ground in a clean mortar as fine powder. Small quantities of glass powder were mixed and ground with KBr in the ratio  $1/25$ . KBr pellets of thickness  $1\text{ mm}$  were formed by pressing the mixture at  $15\text{ tons}$  for a few minutes. All spectra were run at  $4\text{ cm}^{-1}$  resolution.

The Raman spectra were measured in the range  $200$ – $1400\text{ cm}^{-1}$  with a Horiba Jobin Yvon Micro-Raman spectrometer (LABRAM Dilor) coupled to an internal laser He-Ne ( $18\text{ mW}$ ) using the  $632.8\text{ nm}$  line and to an external Spectra-Physics laser  $Ar^+$  ( $200\text{ mW}$ ) using the  $514.5\text{ nm}$  line.

#### 4. Results

The XRD patterns of all glass samples are shown in Fig. 1. The figure exhibits a broad diffuse scattering at low angles instead of crystalline peaks, confirming a long-range structural disorder characteristic of amorphous network.

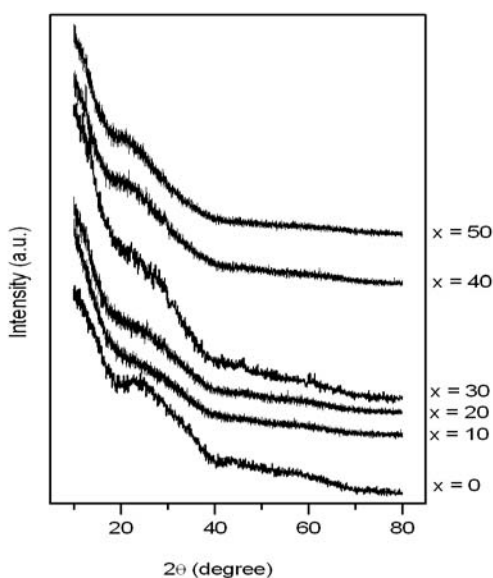


Fig. 1. X-ray diffractograms of  $xV_2O_5$ – $(50-x)CdO$ – $50P_2O_5$  glasses.

Fig. 2 shows the composition dependence of the glass transition temperature  $T_g$  with  $V_2O_5$  content in the  $xV_2O_5$ – $(50-x)CdO$ – $50P_2O_5$  glass system. Two different regimes can be observed in the glass transition temperature variations. For low vanadium oxide concentrations ( $0 \leq x \leq 20$ ),  $T_g$  increases from  $473$  to  $495\text{ }^\circ\text{C}$ . Further increase of  $V_2O_5$  concentration above  $20\text{ mol}\%$  shows a decrease in the glass transition temperature from  $495\text{ }^\circ\text{C}$  in  $20V_2O_5$ – $30CdO$ – $50P_2O_5$  glass to  $440\text{ }^\circ\text{C}$  in  $50V_2O_5$ – $50P_2O_5$  glass.

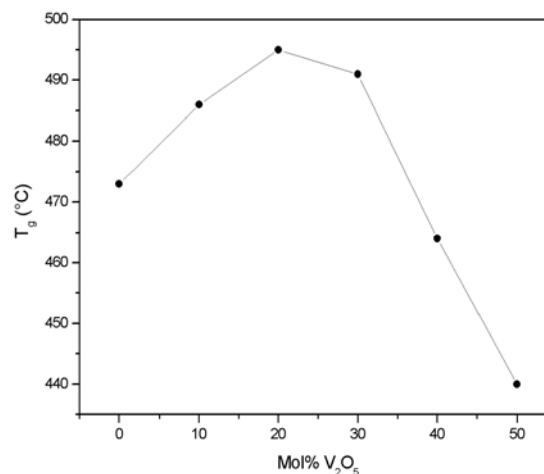


Fig. 2. Composition dependence of glass transition temperature,  $T_g$ , for  $xV_2O_5$ – $(50-x)CdO$ – $50P_2O_5$  glasses.

The FTIR spectra of  $xV_2O_5$ – $(50-x)CdO$ – $50P_2O_5$  glasses ( $0 \leq x \leq 50\text{ mol}\%$ ), in the frequency range between  $400$  and  $1400\text{ cm}^{-1}$  are shown in Fig. 3. The spectrum of the  $50CdO$ – $50P_2O_5$  glass shows a FTIR pattern typical of metaphosphate chain structure [20, 21]. Its characteristic features are the  $PO_2$  asymmetric stretching vibration band at  $1273\text{ cm}^{-1}$ , the  $PO_2$  symmetric stretching vibration band at  $1150\text{ cm}^{-1}$ , the  $\nu_{as}$  of  $PO_3$  groups (chain end) at  $1082\text{ cm}^{-1}$ , the  $\nu_s$  of  $PO_3$  groups at  $1030\text{ cm}^{-1}$ , the  $\nu_{as}$  of POP groups at  $893\text{ cm}^{-1}$ , the  $\nu_s$  of POP groups at  $775$  and  $720\text{ cm}^{-1}$  and the bending vibration ( $\delta$ ) of P–O bonds at  $520$  and  $473\text{ cm}^{-1}$  [22–24].

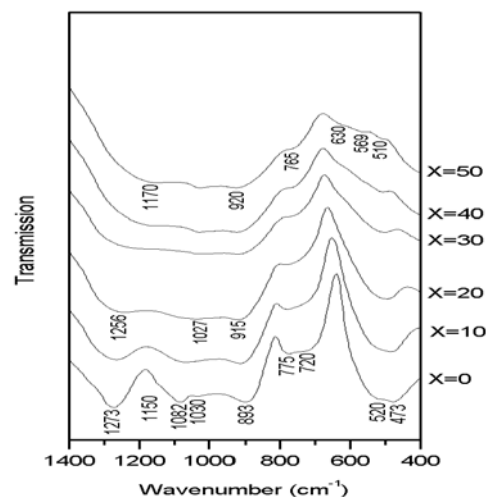


Fig. 3. Infrared spectra of  $xV_2O_5$ – $(50-x)CdO$ – $50P_2O_5$  glasses.

The main feature of the infrared spectra of the glasses with  $0 \leq x \leq 20\text{ mol}\%$   $V_2O_5$  (Fig. 3) is the decrease of the intensity of  $PO_2$  asymmetric stretching vibration band and

of  $\nu_{as}$  and of  $\nu_s$  P–O–P bridges when  $x$  increases from 0 to 20 mol%  $V_2O_5$ . These changes in the spectra of the glasses with  $V_2O_5$  addition are due to the decrease of average phosphate chain length [22]. Absorption band of  $PO_2$  asymmetric stretching mode shifts from  $1273\text{ cm}^{-1}$  in  $50CdO-50P_2O_5$  glass to  $1256\text{ cm}^{-1}$  in  $20V_2O_5-30CdO-50P_2O_5$  glass. The band arising from the P–O–P asymmetric stretching mode shifts to higher frequency from  $893\text{ cm}^{-1}$  (for  $50CdO-50P_2O_5$ ) to  $915\text{ cm}^{-1}$  (for  $20V_2O_5-30CdO-50P_2O_5$ ).

For high vanadium concentrations ( $x \geq 20$  mol%), the  $PO_2$  asymmetric stretching vibration band at  $1256\text{ cm}^{-1}$  for  $x = 20$  mol%  $V_2O_5$  gradually disappears by integration into  $1170\text{ cm}^{-1}$  band in the  $50V_2O_5-50P_2O_5$  glass. This result indicates that no more phosphate chains remain in the glasses with  $x \geq 20$  mol%  $V_2O_5$  [25]. It is interesting to note that the glasses with  $x \geq 20$  mol%  $V_2O_5$  exhibit only a single band at  $765\text{ cm}^{-1}$  which is assigned to the P–O–P linkage in pyrophosphate group ( $P_2O_7^{4-}$ ) [26]. The in-chain P–O–P asymmetric and symmetric decrease in intensity indicating that the number of in-chain P–O–P bonds is diminishing with the increase of  $V_2O_5$  content. Above 10 mol% of  $V_2O_5$  a new band appears at  $1027\text{ cm}^{-1}$ , which gradually increases in intensity with increasing  $V_2O_5$  content. This band is related to the vibrations of isolated V=O vanadyl groups in  $VO_5$  trigonal bipyramids [27, 28]. Dimitrov et al. [1] reported detailed data on the IR spectra of vitreous  $V_2O_5-Bi_2O_3$  ( $20 \leq \text{mol}\% V_2O_5 \leq 100$ ) binary system. They have shown the appearance of one band at  $930\text{ cm}^{-1}$  in  $60V_2O_5-40Bi_2O_3$  glass spectrum which gradually shifts to  $950\text{ cm}^{-1}$  in  $80V_2O_5-20Bi_2O_3$  glass. This band is attributed to the vibrations of the free  $VO_2$  groups of  $VO_4$  tetrahedra, forming chains with V–O–V bridges. This suggests that the absorption band at  $915\text{ cm}^{-1}$  in  $20V_2O_5-30CdO-50P_2O_5$  glass which gradually shifts to  $920\text{ cm}^{-1}$  in  $50V_2O_5-50P_2O_5$  glass could be related to the simultaneous vibrations of P–O–P asymmetric in pyrophosphate groups and  $VO_2$  groups of  $VO_4$  tetrahedra. The bands around  $765\text{ cm}^{-1}$  are broadened in the spectra containing pyrophosphate groups ( $x \geq 20$  mol%  $V_2O_5$ ). The broadened bands can be attributed to the coexistence of the vibrations of P–O–P bridge bonds of  $P_2O_7^{4-}$  groups and the vibrations of V–O bonds of isolated  $VO_4$  groups [29, 30].

At low frequencies, the two bands centered at  $473$  and  $520\text{ cm}^{-1}$  assigned to the bending vibration of ( $\delta$ ) of P–O bonds decrease in intensity and transform into one band centered at  $510\text{ cm}^{-1}$  for higher  $V_2O_5$  content. Results show that the increasing of the  $V_2O_5$  content over 20 mol% decreases the bending harmonics of O=P–O which being replaced with specific vibration of vanadium ions. Thus, this band can be assigned to the combined bending vibrations of V–O [31] and  $PO_4^{3-}$  groups [26]. Above  $x = 20$  mol%  $V_2O_5$ , two weak bands appear at  $569$  and  $630\text{ cm}^{-1}$  which can be attributed to the bending vibrations of V–O [28, 32–34].

The Raman spectra of  $xV_2O_5-(50-x)CdO-50P_2O_5$  glasses ( $0 \leq x \leq 50$  mol%), in the frequency range between 200 and  $1400\text{ cm}^{-1}$  are shown in Fig. 4. The two most intense peaks in the spectrum of the  $50CdO-50P_2O_5$  glass

( $x = 0$  mol%) are due to the symmetric bridging stretching vibrations ( $\nu_s$ ) of the units along the chains at  $696\text{ cm}^{-1}$ , and the terminal P–O stretching vibrations ( $\nu_s$ ) of the  $PO_2$  units at  $1172\text{ cm}^{-1}$  [33]. A second symmetric stretching P–O–P band observed at  $789\text{ cm}^{-1}$  may be due to very short chain phosphate units or ring structures [36, 37]. The lower intensity peak at  $1250\text{ cm}^{-1}$  is the asymmetric  $PO_2$  stretch mode ( $\nu_{as}PO_2$ ) and the small peak at  $1065\text{ cm}^{-1}$  is the symmetric stretch mode  $PO_3$  end groups ( $\nu_sPO_3$ ) [36]. The broad bands at  $330$  and  $500\text{ cm}^{-1}$  are modes most likely involving phosphate bending motions [38]. The frequency of  $PO_2$  asymmetric shifts to lower frequency with increasing  $V_2O_5$  content.

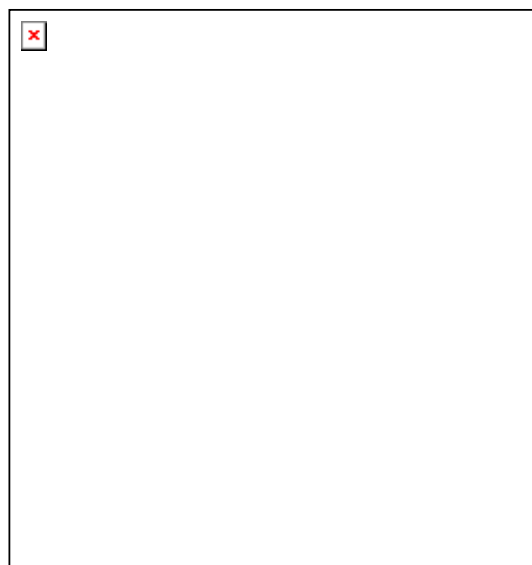


Fig. 4. Raman spectra of  $xV_2O_5-(50-x)CdO-50P_2O_5$  glasses.

Upon addition of vanadium pentoxide to cadmium metaphosphate the following spectra changes are observed: the bands observed around  $696\text{ cm}^{-1}$  and  $1172\text{ cm}^{-1}$  disappear completely when  $x$  reaches 20 mol% and the band observed around  $1250\text{ cm}^{-1}$  disappears for  $x = 50$  mol%. New bands appear at  $615\text{ cm}^{-1}$ ,  $760\text{ cm}^{-1}$ ,  $974\text{ cm}^{-1}$  and  $442\text{ cm}^{-1}$ . The spectrum with the highest vanadium concentration studied ( $x = 50$  mol%) shows a weaker broad band at about  $442\text{ cm}^{-1}$ . This band is assigned to the V–O–V vibrations of metavanadates [39]. The band at  $615\text{ cm}^{-1}$ , which appears for  $x \geq 10$  mol% is assigned to the formation of  $PO_4$  tetrahedral units, bridged through one oxygen to vanadium (V–O– $PO_3$ ) [2]. The spectra with  $x \geq 20$  mol% show a broad band in the  $760-750\text{ cm}^{-1}$  region. This band is assigned to the overlapping V–O–V bridging vibrations which arises by connecting neighboring  $VO_n$  polyhedra through oxygen in the glass [2] and P–O–P bridging vibrations in pyrophosphate groups  $P_2O_7^{4-}$  [38]. The band at  $974\text{ cm}^{-1}$  ( $x = 10$  mol%) which shifts to  $908\text{ cm}^{-1}$  ( $x = 50$  mol%) can be assigned to the V=O vibrations of either tetrahedral  $VO_4$  or trigonal bipyramidal  $VO_5$  [3]. The band in the  $1027-1024\text{ cm}^{-1}$  region is corresponding to

the symmetric  $PO_3$  stretching modes of dimer  $P_2O_7^{4-}$  unit [3, 38].

## 5. Discussion

The evolution of the glass transition temperature can be interpreted from the structural description of the network structure. The maximum in  $T_g$  can be explained by considering changes in the nature of the oxygen bonds that constitute the glass network. The increase in  $T_g$  usually means an increase of the glass rigidity. In the first composition region at low  $V_2O_5$  concentration ( $x \leq 20$  mol%) the glass has the continuous phosphate network. FTIR spectra (Fig. 3) indicate the structural changes of ternary samples with 50 mol%  $P_2O_5$ . Absorption band of  $(PO_2)$  asymmetric stretching mode shifts to lower frequencies as the  $V_2O_5$  content increase. Since the electronegativity of  $V^{5+}$  (1,9 eV) is larger than that of  $Cd^{2+}$  (1,5 eV) [40], we expect that the vanadium–oxygen bond is more covalent than the cadmium–oxygen bond, and the phosphorus–oxygen bonds linked to vanadium ions  $P-O(-V)$  are more ionic than  $P-O(-Cd)$  bonds. Furthermore, the decrease of  $(PO_2)$  asymmetric intensity confirms that  $P-O-Cd$  bonds will be replaced by the  $P-O-V$  bonds when introducing the vanadium oxide. Absorption band of  $P-O-P$  asymmetric stretching mode shifts to higher frequencies as the  $V_2O_5$  content increases. The band shift can be explained by an increase in the covalent fraction of  $P-O-P$  bonds, indicating that the  $P-O-P$  bonds are strengthened with the substitution of  $V_2O_5$  for  $CdO$  [20, 35]. As a result of this,  $T_g$  increases (see Fig. 2). In the second composition region ( $x \geq 20$  mol%), the IR and Raman data show that the structure changes from the continuous phosphate network to the continuous vanadate network by the formation of either tetrahedral  $VO_4$  or trigonal bipyramidal  $VO_5$  with  $V=O$  bonds and short phosphate units such as  $P_2O_7^{4-}$  groups. The main effect observed in IR spectroscopy, with  $V_2O_5$  addition, is the decrease in intensity of the in-chain  $P-O-P$  asymmetric and symmetric indicating that the numbers of in-chain  $P-O-P$  bonds are diminishing with the increase of  $V_2O_5$  content. For the higher  $V_2O_5$  content ( $x = 50$  mol%) the IR and Raman spectra show that the  $V-O$  and  $V-O-V$  vibrations are well observed, indicating that the  $V-O$  and  $V-O-V$  bonds predominate into the glass network. The  $V-O-V$  bond between the  $VO_4$  tetrahedra is less strong than the  $P-O-P$  bond between the  $PO_4$  tetrahedra because the bond strength ( $q/a$ ) of  $V^v$  ( $q/a = 2.65 \text{ \AA}^{-1}$ ) is smaller than that of  $P^v$  ( $q/a = 3.29 \text{ \AA}^{-1}$ ) [40]. Thus, the decreasing of the fraction of the stronger  $P-O-P$  bonds and the increasing of the fraction of the weaker  $V-O-V$  bonds with vanadium oxide addition ( $x \geq 20$  mol%) are responsible for the decrease of  $T_g$ .

## 6. Conclusions

The composition dependence of  $T_g$ , infrared spectroscopy and Raman spectroscopy of the  $xV_2O_5$ –(50-

$x$ ) $CdO$ –50 $P_2O_5$  glass system over the compositional range  $0 \leq x \leq 50$  mol% show that the rigidity of the vitreous matrix is related to the manner in which  $V_2O_5$  gets arranged in the glass. For low vanadium oxide concentrations ( $x \leq 20$  mol%), FTIR and Raman spectra reveal the formation of  $P-O-V$  bonds, which increase the cross-link strength of the glass network and leads to increased  $T_g$ . In the high  $V_2O_5$  concentration range ( $x > 20$  mol%), the vanadium oxide plays the role of a second glass former and it is evolved from a phosphate network to a vanadophosphate network where pyrophosphate groups  $(P_2O_7)^{4-}$  can be detected. The vanadium takes part in the network of the glasses as  $VO_5$  and  $VO_4$  groups forming chains with  $V-O-V$  bridges. The increasing of the fraction of the weaker  $V-O-V$  bonds and the diminishing of the numbers of the stronger in-chain  $P-O-P$  bonds with the increase of  $V_2O_5$  concentration decrease the glass network connectivity, in accordance with the decrease of  $T_g$ .

## References

- [1] V. Dimitrov, Y. Dimitriev, A. Montenero, *J. Non-Cryst. Solids* **180**, 51 (1994).
- [2] A. Chrissanthopoulos, C. Pouchan, G. N. Papatheodorou, *Z. Naturforsch.* **56a**, 773 (2001).
- [3] I. Ardelean, C. Andronache, C. Cîmpean, *Mod. Phys. Lett.* **B20** (2&3), 105 (2006).
- [4] I. Ardelean, D. Rusu, C. Andronache, V. Ciobotă, *Mater. Lett.* **61**, 3301 (2007).
- [5] N. Vedeanu, O. Cozar, I. Ardelean, B. Lendl, D. A. Magdas, *Vibrational Spectroscopy* **48**, 259 (2008).
- [6] M. S. Al-Assiri, *Physica B, Cond. Mat.* **403**, 2684 (2008).
- [7] R. V. S. S. N. Ravikumar, V. Reddy, A. V. Chandrasekhar, B. J. Reddy, Y. P. Reddy, P. S. Rao, *J. Alloys Compd.* **337**, 272 (2002).
- [8] J. E. Garbarczyk, M. Wasiucioneck, P. Macowski, W. Takubowski, *Solid State Ionics* **119**, 19 (1999).
- [9] H. Hirashima, T. Yoshida, D. Arai, *J. Am. Ceram. Soc.* **68**(9), 486 (1985).
- [10] F. E. Salman, N. Shashy, H. Abou El-Haded, M. K. El-Mansy, *Phys. Chem. Glasses* **63**, 1957 (2001).
- [11] S. Stizza, I. Davoli, O. Gzowski, L. Murawski, M. Tomellini, A. Marcelli, A. Bianconi, *J. Non-Cryst. Solids* **80**, 175 (1986).
- [12] F. R. Landsberger, P. J. Bray, *J. Chem. Phys.* **53**, 2757 (1970).
- [13] O. Attos, M. Massot, M. Balkanski, E. Haro Poniowski, M. Asomoza, *J. Non-Cryst. Solids* **210**, 163 (1997).
- [14] L. Murawski, R. J. Barczyński, *J. Non-Cryst. Solids* **196**, 275 (1996).
- [15] S. Sindhu, S. Sanghi, S. Rani, A. Agarwal, V. P. Seth, *Mater. Chem. Phys.* **107**, 236 (2008).
- [16] V. Dimitrov, *J. Non-Cryst. Solids* **192 & 193**, 183 (1995).

- [17] D. Bersani, G. Antonioli, P. P. Lottici, Y. Dimitriev, V. Dimitrov, P. Kobourova, *J. Non-Cryst. Solids* **232–234**, 293 (1998).
- [18] C. Mercier, G. Palavit, L. Montagne, C. Follet-Houttemane, *C.R. Chimie* **5**, 693 (2002).
- [19] A. Chahine, M. Et-tabirou, M. Elbenaissi, M. Haddad, J. L. Pascal, *Mater. Chem. Phys.* **84**, 341 (2004).
- [20] P. Y. Shih, S. W. Yung, T. S. Chin, *J. Non-Cryst. Solids* **244**, 211 (1999).
- [21] A. Chahine, M. Et-tabirou, *Ann. Chim. Sci. Mat.* **28**, 25 (2003).
- [22] D. E. C. Corbridge, J. E. Lowe, *J. Chem. Soc., Part I*, 493 (1954).
- [23] C. Garrigou-Lagrange, M. Ouchetto, B. El Ouadi, *Canad. J. Chem.* **63**, 1436 (1985).
- [24] R. F. Bartholomew, *J. Non-Cryst. Solids* **7**, 221 (1972).
- [25] A. Chahine, M. Et-tabirou, M. Elbenaissi, M. Haddad, J. L. Pascal, *Mater. Chem. Phys.* **84**, 341 (2004).
- [26] C. Dayanand, G. Bhikshamaiah, V. Jaya Tayagaraju, M. Salagram, A. S. R. Krishna Murthy, *J. Mat. Sci.* **31**, 1945 (1996).
- [27] E. Dachille, R. Roy, *J. Am. Ceram. Soc.* **42**, 78 (1965).
- [28] R. Iordanova, Y. Dimitriev, V. Dimitrov, S. Kassabov, D. Klissurski, *J. Non-Cryst. Solids* **204**, 141 (1996).
- [29] K. Nakamoto, *Infrared Spectra of Inorganic and Coordination Compounds* (Wiley, New York, 1964).
- [30] R. Nyquist, R. Kagel, *Infrared Spectra of Inorganic and Coordination Compounds*, Academic Press, New York 10 (1971).
- [31] D. Ilieva, V. Dimitrov, Y. Dimitriev, *Phys. Chem. Glasses* **38(2)**, 79 (1997).
- [32] T. Gilson, O. Bizri, N. Cheetham, *J. Chem. Soc. Dalton Trans. Inorg. Chem. A* 291 (1973).
- [33] L. Abello, E. Husson, Y. Replin, G. Lucazeau, *Spectrochim. Acta* **39A**, 641 (1983).
- [34] Y. Dimitriev, M. Arnaudov, V. Dimitrov, *Mh. Chem.* **107**, 1335 (1976).
- [35] M. El Hezzat, M. Et-Tabirou, L. Montagne, E. Bekaert, G. Palavit, A. Mazzah, P. Dhamelincourt, *Mater. Lett.* **58**, 60 (2003).
- [36] J. E. Pemberton, L. Latizadeh, J.P. Feltcher, S. H. Risbud, *Chem. Mater.* **3**, 195 (1991).
- [37] H.S. Liu, P.Y. Shih, T.S. Chin, *Phys. Chem. Glasses* **38(3)**, 123 (1997).
- [38] R. K. Brow, D. R. Tallant, W. L. Warren, A. MacIntyre, D. E. Day, *Phys. Chem. Glasses* **38(6)**, 300 (1997).
- [39] T. Hübner, G. Mosel, K. Witke, *Glass Phys. Chem.* **27**, 114 (2001).
- [40] M. B. Volf, *Chemical Approach to Glass, Glass Science and Technology*, Elsevier, Vol. 7 (1984).

\*Corresponding author: kerkourinaj@hotmail.com;  
kerkouri-najia@univ-ibntofail.ac.ma